Analysis, design, and control of standalone PV based boost DC-AC converter

Jnanaranjan Nayak[1], Sunil Kumar[1], Pradeep Kumar Sahu[2], Satyaranjan Jena[2]

[1]Department of Electrical Engineering, Kalinga University, Naya Raipur, Chhattisgarh, India
[2]School of Electrical Engineering, Kalinga Institute of Industrial Technology Deemed to be University, Bhubaneswar, India

Article Info	ABSTRACT
	This paper presents a new control scheme for a boost DC–AC converter which is used for solar power applications. The proposed DC-AC converter configuration can produce an AC voltage level across the output or load side greater than input DC voltage based on the operating duty cycle. Generally, the conventional DC-AC converter or voltage source inverter (VSI) generates AC voltage which is less than input DC voltage. Maintaining a constant voltage across the load with improved dynamic performance is challenging for anyone for the solar photovoltaic (PV) system. A dual-loop sliding mode control is proposed for the boost VSI to address the above issues. The proposed controller has robust in nature against the wide fluctuation in the plant or load parameters. The design, analysis and control of the boost DC-AC converter are briefly discussed in this paper. This topology can be broadly used in solar powered uninterruptible power supply (UPS) where boosting operation is essential for low voltage solar PV system. This topology eliminates the DC boosting power processing stage which leads an improved efficiency of the overall system. The MATLAB/Simulink results are presented to highlight the above issues. *This is an open access article under the CC BY-SA license.*

Corresponding Author:

Satyaranjan Jena
School of Electrical Engineering, Kalinga Institute of Industrial Technology Deemed to be University
Patia, Bhubaneswar, Odisha 751024, India
Email: srj.kiit@gmail.com

1. INTRODUCTION

The electricity demand is considered as the promising measure the living standard quality of the people for any developing country. The economic growth of the country also depends upon the electricity demand. However, the major problem faced by the human society in the present day is the shortage of the electricity. This leads to the generation of green energy such as: solar energy, and wind energy, as the power generation from the conventional sources produce major pollutions for the environments. The non-conventional sources are clean as well as free from the greenhouse effect. Generally, power generated from the solar PV system is commonly used due to its low cost, robust in nature and freely available at any location of the globe [1], [2]. Now-a-days stand-alone PV system gains more attention in rural India, where the grid availability is not possible due to its demographic location. A stand-alone photovoltaic (PV) system comprises of solar PV panels, DC-DC converter for boosting the low voltage produced by the PV panel, DC-AC converter or voltage source inverter (VSI) to convert DC power to AC power, a critical load, and a storage unit. However, the operation of storage unit is not discussed in this paper for the simplicity purpose. This paper only provides the design guidelines for the boost VSI by eliminating any DC power conversion stage.

Various inverter techniques are employed in solar photovoltaic (SPV) systems. One of the traditional approaches is the voltage source inverter (VSI) equipped with a boosting unit. This conventional method can be achieved through a range of approaches, as:

- The application of a step-up transformer serves to elevate the voltage. Nevertheless, this technique results in an enlargement of the system's dimensions, expenses, and mass due to the incorporation of a line to frequency transformer.
- An alternative involves the utilization of a high-frequency transformer (HFT) integrated with dual conversion stages to amplify the input voltage. This strategy is executed through a boost DC-DC converter trailed by an inverter.
- Employing an HFT alongside a rectified sinusoidal wave modulated DC-DC converter, which is subsequently expanded through a cyclo converter.

Numerous sources in the literature [3]–[8] explore different configurations involving high-frequency transformers. Nonetheless, many of these setups achieve high voltage gain by altering the transformer turns ratio, leading to substantial current ripples in converters. This phenomen on could ultimately have a negative impact on the operational longevity of solar PV panels. In response to this concern, isolated current-fed converters have been applied, including the push–pull converter [9], full-bridge converters [10], and half-bridge converters [11]. However, the implementation of these approaches introduces challenges such as heightened intricacy, increased weight, elevated expenses, and diminished efficiency and lifespan. To mitigate expenses, reduce weight, and enhance both flexibility and efficacy, researchers have proposed transformerless topologies as an alternative solution [4], [5]. Therefore, transformerless inverters are considered suitable for a photovoltaic system.

Generally, the conventional VSI generates an AC output voltage which is always lower than the input DC power. Therefore, DC-DC converter is used in between the input DC side and the VSI to step-up the DC voltage as shown in Figure 1. However, this additional DC-DC converter makes the system bulky, more costly with low efficiency [5], [6]. In this paper, a new topology of VSI is designed for the solar PV system which has higher AC voltage than the input DC voltage.

The fast dynamic response and improved steady state performance is highly essential for VSI [7], [8]. These issues are briefly addressed in the literature by designing an appropriate control scheme. The various controllers are used to improve the steady-state and dynamic response such as: repetitive control [9], [10], hysteresis control [11], [12], deadbeat control [13], internal model control [14], multi-loop feedback control [15], [16]. However, these controllers are operated on the principle of average model of the VSI. The dynamic equation of the VSI will change with change in the switching states. In these controllers, the duty cycle of VSI switch is approximated over a small interval of the time. Therefore, the abovesaid control scheme can efficiently operate around its operating point only. A non-linear current controller, also called sliding mode control (SMC) is suitable for the VSI due to its robust nature, simple design, and low cost. The SMC does not require the average model of the system [17]–[19].

The SMC can be designed by taking a robust sliding surface and a switching scheme to improve both the steady-state and dynamic performance of the VSI. The salient features of the proposed SMC for boosting VSI can be summarized as follows: i) inherent robust features for wide variation of load and line parameters, ii) fast dynamic response, iii) Low settling time, and iv) Relatively low voltage overshoots under wide variation in the local load conditions. In this paper, a high performance and fixed frequency SMC is designed for a single phase VSI. A pulse width modulation (PWM) technique is used for keeping a constant frequency and generates the control pulses for the switches of VSI.

2.   INVERTER TOPOLOGY AND OPERATING PRINCIPLES

In this proposed topology, the load is connected differentially across two converters as shown in Figure 2. The output DC biased voltage across the converter 1, V_1 is shown in Figure 3(a) and converter 2, V_2 is shown in Figure 3(b). The AC sinusoidal output voltage of the proposed converter is taken across the two DC-DC converters (converter 1 and 2). The principle of the operation of the proposed boost inverter is similar to the Cuk converter [20]. The DC-DC converters generate an output AC sinusoidal voltage with s DC-biased voltage which results a unipolar voltage. The voltage generated by these two DC-DC converters is 180-degree phase with each other. These two voltages additive in nature across the load.

The voltages of the converter can be calculated by taking average method during the continuous conduction mode of operation as shown in Figure 3. The boost ratio for the proposed converter, the output voltage of the boost inverter derived by taking 180 degrees out of the phase of two DC-DC converter voltage. The proposed converter yields a zero-output voltage when the duty cycle is 0.5, as illustrated in (3). Hence, operating the duty cycle around this point allows for the generation of an output voltage.

$$\frac{V_1}{V_{in}} = \frac{1}{1-d} \tag{1}$$

$$V_0 = V_1 - V_2 = \frac{V_{in}}{1-d} - \frac{V_{in}}{d} \tag{2}$$

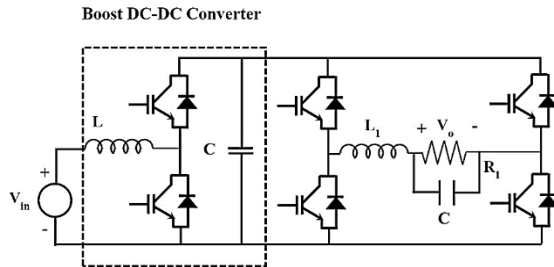$$\frac{V_0}{V_{in}} = \frac{2d-1}{d(1-d)} \tag{3}$$

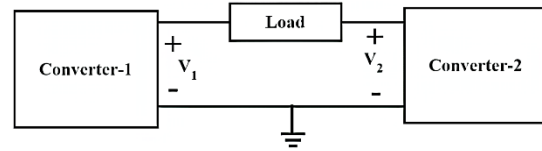Figure 1. Conventional single-phase boost DC-AC converter
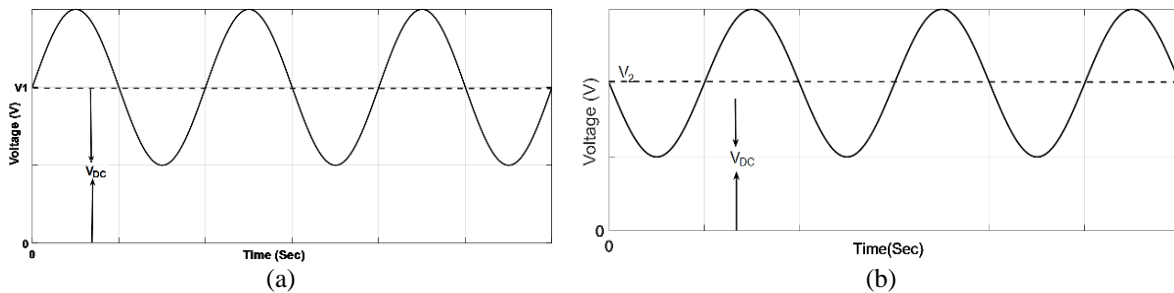
Figure 2. Fundamental approach of boost inverter

Figure 3. Output DC-biased voltage across (a) converter 1 and (b) converter 2

3. CONTROL SCHEME FOR BOOST VSI

The appropriate controller is designed for the boost VSI to improve both the steady state and dynamic performance. The steady state performance can be evaluated for the inverter in terms of total harmonic distortion (THD) level of the output voltage. The output voltage of the VSI should have a THD level as decided by the IEEE standard 1947 [21]–[23]. The detailed standards and regulations are further briefly reported in [24], [25]. Similarly, the dynamic performance can be evaluated under large load fluctuations. These issues of VSI can be addressed by employing a non-linear control called sliding mode control (SMC). The proposed SMC has two control loops. The outer voltage loop is used to improve the steady state performance whereas the dynamic performance of VSI can be enhanced by the inner current control. Both the control loops of SMC comprise a conventional proportional-integral (PI) controller to minimize the error.

3.1. System description

The proposed boost VSI topology is shown in Figures 2 and 3. It comprises of a constant DC source which is equivalent to the output voltage generated by an ideal solar PV system, filter inductor, storage capacitors, controlled power switches, free-wheeling diode, and a resistive load. Here, both sides of VSI are employed by two SMC scheme. The function of these two controllers is to track the voltage across two capacitor C_1 and C_2 and exactly follow the reference AC voltage as decided by the user. The working principle of the boost inverter can be explained by the bidirectional current DC-DC boost converter as shown in Figure 4. The proposed boost converters are analyzed under the ideal conditions and the operation of the converter is assumed in the continuous conduction mode. The turn-on and turn-off conditions of the proposed converter can be derived from the equivalent diagram.

For the right-hand side of the converter topology as shown in Figure 5. When the switch S_1 and S_2 are turn-on and turn-off respectively then the current through the inductor is linearly increases and the diode D_1 is in reverse biased conditions. In this condition, the capacitor C_1 delivers the voltage to the load and the voltage V_1 gradually decreases. On the other hand, when the switch S_1 and S_2 are turn-off and turn-on respectively, the capacitor C_1 is charged by the current i_1. The dynamic equations of the boost inverter by taking the states i_1 and V_1 are given by (4).

$$\dot{x} = Ax + Bu + C$$
$$x = \begin{pmatrix} i_1 \\ v_1 \end{pmatrix}, \quad A = \begin{pmatrix} \frac{-R_a}{L_1} & -\frac{1}{L_1} \\ \frac{1}{C_1} & -\frac{1}{C_1 R_1} \end{pmatrix}, \quad B = \begin{pmatrix} \frac{V_1}{L_1} \\ \frac{-i_1}{C_1} \end{pmatrix}, \quad C = \begin{pmatrix} \frac{V_{in}}{L_1} \\ \frac{-V_2}{C_1 R_1} \end{pmatrix} \tag{4}$$

Where u is the switching states of the inverter, x and dx/dt are the state vector and its derivatives.

$$u = \begin{cases} 1 \rightarrow S_1 \text{ is ON and } S_2 \text{ is OFF} \\ 0 \rightarrow S_1 \text{ is OFF and } S_2 \text{ is ON} \end{cases} \tag{5}$$
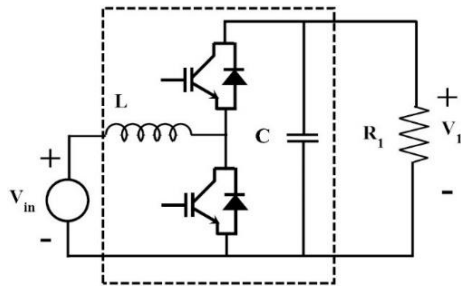

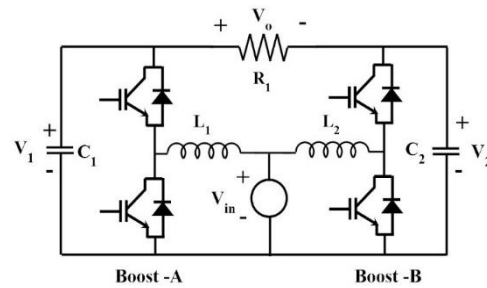Figure 4. Bidirectional step-up DC-DC converter

Figure 5. Proposed boost DC-AC converter topology

3.2. Sliding mode control for boost inverter

In the first step, the proposed SMC can be designed by taking a stable sliding surface in terms of state variables of the system as shown in Figure 6. The voltage and current error are taken as the state variables for the system. The error signals are generated by comparing the feedback signal with its reference value. The sliding surface for the inverter is given by (6).

$$S(i_1, V_1) = K_1 e_1 + K_2 e_2 \tag{6}$$

Where K1 and K2 are positive constants, called sliding coefficients and the values are calculated as per [16] and the state variables are given by (7) and (8).

$$e_1 = i_{1ref} - i_1 \tag{7}$$

$$e_2 = V_{1ref} - V_1 \tag{8}$$

The sliding mode control can be expressed in terms of state variables as (9).

$$S(i_1, V_1) = K_1(i_{1ref} - i_1) + K_2(V_{1ref} - V_1) \tag{9}$$

In the second step, the SMC uses a switching control law to drive the state trajectory from any initial positions to the sliding surface. In this paper, a hysteresis band or a relay block is used for control signal generation.

In the SMC, the state variables are taken by sensing the current and voltage and the errors are generated by subtracting it from the reference value. But, the generation of inductor current reference is difficult as its value depends on the output load and the input voltage. However, this problem can be overcome by passing the inductor current error in a high-pass filter. In this case, the low frequency component of the current error is adjusted by the inverter operation. Therefore, the high frequency variables

are only controlled by the proposed SMC. The system now becomes more complex because the order increased by introducing the high-pass filter. The above problem can be avoided by selecting filter cut-off frequency which is smaller than the switching frequency [10].
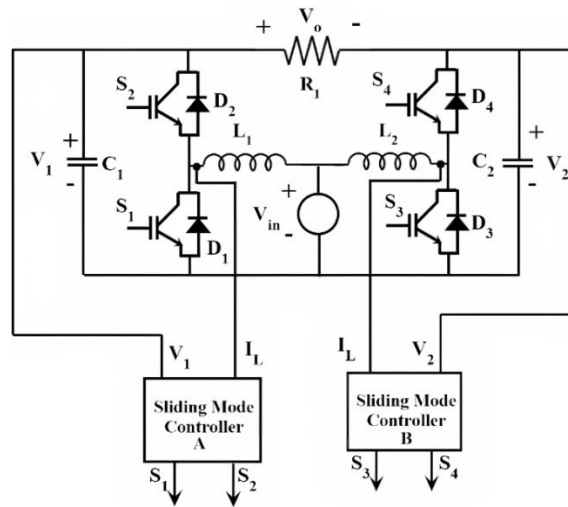

Figure 6. Control block diagram of proposed boost inverter

4. DESIGN GUIDELINES

The various design parameters for the boost inverter are discussed in this section. These component parameters are helpful for designing the prototype model. The detailed design parameter is calculated by referring [13]. The designed boost inverter specifications are given in Table 1.

Table 1. Boost inverter specifications

S.L.	Parameter	Rating
1	Required output power	1000 W
2	Output load voltage	230 V
3	Input voltage to inverter	150 V
4	Line frequency	50 Hz
5	Boost inverter Switching frequency	30 kHz

4.1. Calculation of capacitor voltages V_{01} and V_{02}

The output voltage of the inverter topology is given as (10).

$$V_0 = V_1(t) - V_2(t) = 180\sin(314t) \tag{10}$$

As shown in Figure 3, the output voltage of converter A and B are opposite phase with each other, both the output voltages are given by (11).

$$V_1(t) = V_{dc} + 90\sin(314t)$$
$$V_2(t) = V_{dc} - 90\sin(314t) \tag{11}$$

By taking the DC supply voltage Vdc=235 V, the (11) can be rewritten as (12).

$$V_1(t) = 235 + 90\sin(314t)$$
$$V_2(t) = 235 - 90\sin(314t) \tag{12}$$

4.2. Calculation of L_1 and C_1

The acceptable level of ripple current through the inductor is selected as 20% as defined by the IEEE standard 1947 [16]. By taking the above consideration, the inductor value is chosen as 800 µH. The

capacitor value is selected based on the maximum voltage ripples for a particular application. The acceptable level of ripple output voltage for the inverter is equals to 5% of the rated voltage. For this application, the ripple voltage is taken as 10 V (peak to peak). From. One can calculate C1>38.7 µF. The capacitor for this boost inverter is chosen as 40 µF [13].

4.3. Calculation of control; parameter K₁ and K₂

The steady and dynamic response of the system depends on the control parameters K1 and K2. These are the positive real constant and called sliding co-efficient. The parameters can be determined by [16]. The improper tuning of the parameters leads the power quality issues like inductor ripple current, capacitor ripple voltage, switching frequency, and stability of the system. Table 2 presents a comparative analysis of few selected single-phase inverter topologies, organized according to their component count, voltage gain, controller type, and switching frequency [26]–[29].

Table 2. Comparison of single-phase boost inverter topologies

Ref.	No. of components				V_{in} (V)	V_{orms} (V)	Voltage gain	L_f (mH)	C_f (µF)	Controller	f_{sw} (kHz)
	S	D	C	L							
[26]	4	4	2	3	80	110	NA	20	10	Carrier based PWM	4
[27]	5	2	1	1	65	110	M/(1-2d)	10	4.6	SPWM	9.5
[28]	5	5	1	2	68	127	(1+d)/(1-3d)	20	3	SPWM	10
[29]	8	1	3	1	80	110	NA	NA	NA	SPWM	35
Proposed method	4	0	2	2	100	157	(2d-1)/d(1-d)	80	500	Sliding mode	30
S: No. of switches; D: No. of diodes; C: No. of capacitors; and L: No. of inductors											

5.   SIMULATION RESULTS

In order to demonstrate the performance of the proposed boost inverter topology, the model has been simulated by MATLAB/Simulink. The detailed plant parameters and control parameters considered in this paper. The LC filter is designed by taking the resonant frequency of 3 kHz. The boost inverter is designed for a switching frequency of 20 kHz and 1 kVA rating. The control parameters are tuned to attain the best steady and dynamic performance of the system. The steady state performance is evaluated in terms of THD and the dynamic response of the system is evaluated step load change.

The steady-state performance: First the steady-state performance of the boost inverter is evaluated by taking resistive load. The output voltage and the load current are shown in Figure 7(a) and its THD is represented by the Figure 7(b). The line current is very closed to sine waveform and operated with unity power factor with the output voltage. The THD level of the output voltage is measured and found to be 2.75% which is allowed by the IEEE 1947. The steady-state performance is also evaluated by inserting an uncontrolled rectifier non-linear load in between boost inverter and load as shown in Figure 8. Figure 9(a) shows the output voltage and load current for non-linear load whereas the THD of the output voltage is shown in Figure 9(b). From the Figure 9, it can be concluded that although the current is heavily distorted but the load voltage suffers a little distortion.

The dynamic performance of the boost inverter is evaluated under step load change by connecting or disconnecting parallel load. Figure 10(a) shows the output voltage and load current for a step load change in no-load to full load. It can be concluded that the load current quickly settles from old operating point to new operating point. The load variation from full-load to no-load is repeated and shown in Figure 10(b). The performance of the proposed controller is compared with its counterparts and summarized in Table 3.
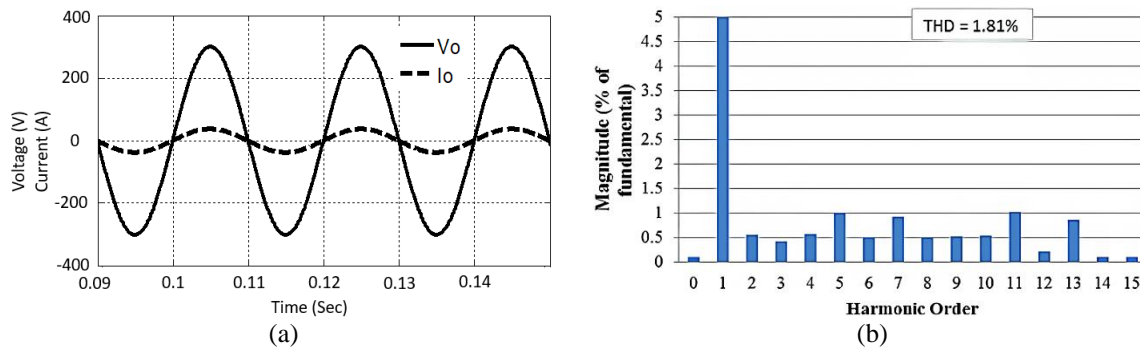

Figure 7. Steady-state performance under resistive load (a) output voltage and current and (b) output voltage THD
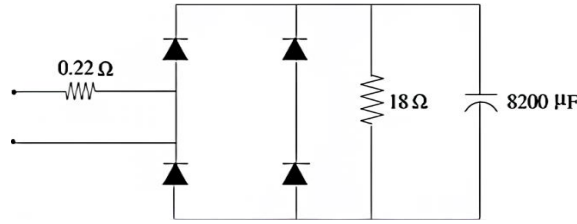
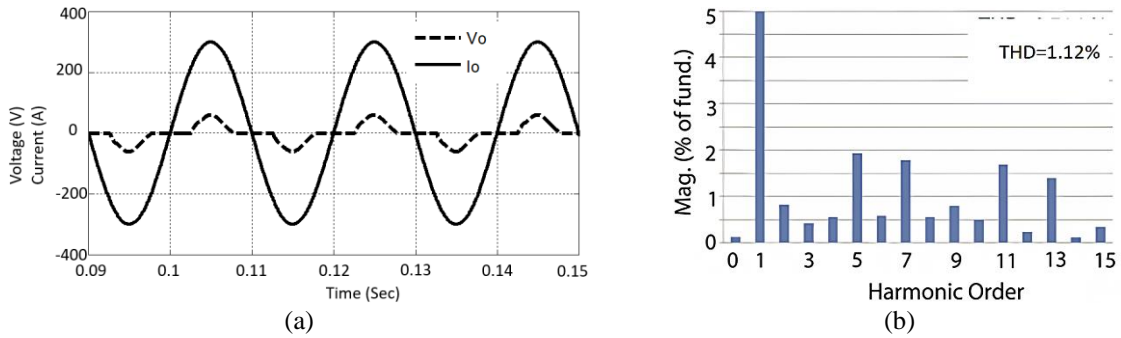Figure 8. Uncontrolled rectifier non-linear load

Figure 9. Steady-state performance under non-linear load (a) output voltage and current
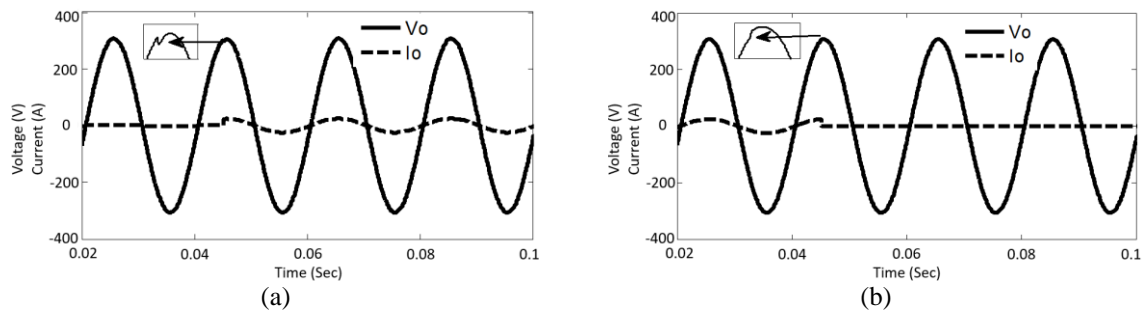and (b) output voltage THD

Figure 10. Transient performance of boost inverter (a) no-load to full load and (b) full-load to no-load

Table 3. Comparison of performance parameters of the single-phase boost inverter topologies

Ref.	Efficiency (%)	Power factor	THD (%)
[26]	93.2	0.99	4.42
[27]	95	1	2.773
[28]	95	0.996	4
[29]	80	0.99	5
Proposed method	96.5	1	2

6.   CONCLUSION

The theoretical analysis and design of a new boost DC-AC converter topology is briefly discussed here. The sliding mode control is employed for controlling the proposed boost inverter to improve the steady and dynamic response. The output voltage has low THD level of 2.75% and 3.17% for the resistive and non-linear load respectively which ensures the steady state performance of the proposed controller. The proposed controller has also good dynamic response under large load variations. The proposed topology can commonly be employed for the application where higher output AC voltage is required from a low DC-voltage. The topology has applications in solar PV system which eliminates any DC-DC boosting stage or UPS system.

REFERENCES

[1]   S. Chu and A. Majumdar, "Opportunities and challenges for a sustainable energy future," *Nature*, vol. 488, no. 7411, pp. 294–303, Aug. 2012, doi: 10.1038/nature11475.

[2]   N. Kannan and D. Vakeesan, "Solar energy for future world: - A review," *Renewable and Sustainable Energy Reviews*, vol. 62, pp. 1092–1105, Sep. 2016, doi: 10.1016/j.rser.2016.05.022.

[3]   M. Biswas, S. P. Biswas, M. R. Islam, M. A. Rahman, K. M. Muttaqi, and S. M. Muyeen, "A new transformer-less single-phase photovoltaic inverter to improve the performance of grid-connected solar photovoltaic systems," *Energies*, vol. 15, no. 22, p. 8398, Nov. 2022, doi: 10.3390/en15228398.

[4]   R. Gonzalez, J. Lopez, P. Sanchis, and L. Marroyo, "Transformerless inverter for single-phase photovoltaic systems," *IEEE Transactions on Power Electronics*, vol. 22, no. 2, pp. 693–697, Mar. 2007, doi: 10.1109/TPEL.2007.892120.

[5]   M. M. Z. Moustafa, M. Aboushal, T. EL-Fouly, A. Al-Durra, and H. Zeineldin, "A novel unified controller for grid-connected and islanded operation of PV-fed single-stage inverter," *IEEE Transactions on Sustainable Energy*, vol. 12, no. 4, pp. 1960–1973, Oct. 2021, doi: 10.1109/TSTE.2021.3074248.

[6]   I. Vairavasundaram, V. Varadarajan, P. J. Pavankumar, R. K. Kanagavel, L. Ravi, and S. Vairavasundaram, "A review on small power rating PV inverter topologies and smart PV inverters," *Electronics*, vol. 10, no. 11, p. 1296, May 2021, doi: 10.3390/electronics10111296.

[7]   A. Comacchio, G. Bonanno, H. Abedini, P. Mattavelli, and M. Corradin, "Asymmetric digital dual-edge modulator for dynamic performance improvement of multiloop-controlled VSI," *IEEE Transactions on Industrial Electronics*, vol. 70, no. 5, pp. 4662–4671, May 2023, doi: 10.1109/TIE.2022.3187586.

[8]   P. K. Pardhi and S. Sharma, "Implementation of robust controller for VSI feeding stand-alone loads," in *2019 IEEE 1st International Conference on Energy, Systems and Information Processing (ICESIP)*, Jul. 2019, pp. 1–5. doi: 10.1109/ICESIP46348.2019.8938247.

[9]   K. Mahmud and G. E. Town, "A review of computer tools for modeling electric vehicle energy requirements and their impact on power distribution networks," *Applied Energy*, vol. 172, pp. 337–359, Jun. 2016, doi: 10.1016/j.apenergy.2016.03.100.

[10] N. Moeini, M. Bahrami-Fard, M. Shahabadini, S. M. Azimi, and H. Iman-Eini, "Passivity-based control of single-phase cascaded H-bridge grid-connected photovoltaic inverter," *IEEE Transactions on Industrial Electronics*, vol. 70, no. 2, pp. 1512–1520, Feb. 2023, doi: 10.1109/TIE.2022.3165266.

[11] W. Zhifu, W. Yupu, and R. Yinan, "Design of closed-loop control system for a bidirectional full bridge DC/DC converter," *Applied Energy*, vol. 194, pp. 617–625, May 2017, doi: 10.1016/j.apenergy.2016.11.113.

[12] D. Chen, J. Zhang, and Z. Qian, "An improved repetitive control scheme for grid-connected inverter with frequency-adaptive capability," *IEEE Transactions on Industrial Electronics*, vol. 60, no. 2, pp. 814–823, Feb. 2013, doi: 10.1109/TIE.2012.2205364.

[13] A. Lunardi, E. Conde, J. Assis, L. Meegahapola, D. A. Fernandes, and A. J. Sguarezi Filho, "Repetitive predictive control for current control of grid-connected inverter under distorted voltage conditions," *IEEE Access*, vol. 10, pp. 16931–16941, 2022, doi: 10.1109/ACCESS.2022.3147812.

[14] S. Lavanya, S. Prabakaran, and R. Malathi, "Hysteresis controlled interleaved boost converter - Inverter system in real time for wind generator applications," 2022, p. 020033. doi: 10.1063/5.0127321.

[15] D. J. P. Roselyn, D. Sen, P. Lal, N. P. Purkayastha, and C. Nithya, "Development of hysteresis current controller for power quality enhancement in grid connected PV system," *International Journal of Electrical Engineering and Technology*, vol. 11, no. 4, pp. 8–21, 2020, doi: https://ssrn.com/abstract=3656988.

[16] B. R. V S and G. G. Devadhas, "Design and development of new control technique for standalone PV system," *Microprocessors and Microsystems*, vol. 72, p. 102888, Feb. 2020, doi: 10.1016/j.micpro.2019.102888.

[17] S. R. Mohapatra, P. Sekhar, V. Agarwal, and S. C. Patwardhan, "Experimental evaluation of internal model control for 3φ grid-tied solar PV inverter," in *2020 International Conference on Power Electronics & IoT Applications in Renewable Energy and its Control (PARC)*, Feb. 2020, pp. 432–436. doi: 10.1109/PARC49193.2020.236647.

[18] B. Pal, P. K. Sahu, and S. Mohapatra, "A review on feedback current control techniques of grid-connected PV inverter system with LCL filter," in *2018 Technologies for Smart-City Energy Security and Power (ICSESP)*, Mar. 2018, pp. 1–6. doi: 10.1109/ICSESP.2018.8376682.

[19] S. Roy, P. K. Sahu, and S. Jena, "Analysis and control strategy of standalone PV system with various reference frames," *Open Engineering*, vol. 12, no. 1, pp. 616–626, Oct. 2022, doi: 10.1515/eng-2022-0371.

[20] B. Sahoo, S. K. Routray, and P. K. Rout, "Execution of robust dynamic sliding mode control for smart photovoltaic application," *Sustainable Energy Technologies and Assessments*, vol. 45, p. 101150, Jun. 2021, doi: 10.1016/j.seta.2021.101150.

[21] D. K. Dash, P. K. Sadhu, and B. Subudhi, "Photovoltaic grid management systems with sliding mode control," *Microsystem Technologies*, vol. 28, no. 12, pp. 2775–2783, Dec. 2022, doi: 10.1007/s00542-022-05349-x.

[22] K. Chigane and M. Ouassaid, "Voltage and power control for a grid tied single phase single stage transformer-less photovoltaic system using sliding mode control," in *WITS 2020*, 2022, pp. 687–697. doi: 10.1007/978-981-33-6893-4_63.

[23] R. Kumar and B. Singh, "Solar PV array fed cuk converter-VSI controlled BLDC motor drive for water pumping," in *2014 6th IEEE Power India International Conference (PIICON)*, Dec. 2014, pp. 1–7. doi: 10.1109/POWERI.2014.7117669.

[24] Y.-K. Wu, J.-H. Lin, and H.-J. Lin, "Standards and guidelines for grid-connected photovoltaic generation systems: A review and comparison," *IEEE Transactions on Industry Applications*, vol. 53, no. 4, pp. 3205–3216, Jul. 2017, doi: 10.1109/TIA.2017.2680409.

[25] X. Zhang, X. Zhao, S. Smith, J. Xu, and X. Yu, "Review of R&D progress and practical application of the solar photovoltaic/thermal (PVT) technologies," *Renewable and Sustainable Energy Reviews*, vol. 16, no. 1, pp. 599–617, Jan. 2012, doi: 10.1016/j.rser.2011.08.026.

[26] B. N. Alajmi, K. H. Ahmed, G. P. Adam, and B. W. Williams, "Single-phase single-stage transformer less grid-connected PV system," *IEEE Transactions on Power Electronics*, vol. 28, no. 6, pp. 2664–2676, Jun. 2013, doi: 10.1109/TPEL.2012.2228280.

[27] S. S. Nag and S. Mishra, "Current-fed switched inverter," *IEEE Transactions on Industrial Electronics*, vol. 61, no. 9, pp. 4680–4690, Sep. 2014, doi: 10.1109/TIE.2013.2289907.

[28] M. Nguyen, T. Le, S. Park, Y. Lim, and J. Yoo, "Class of high boost inverters based on switched-inductor structure," *IET Power Electronics*, vol. 8, no. 5, pp. 750–759, May 2015, doi: 10.1049/iet-pel.2014.0471.

[29] P. K. Peter and V. Agarwal, "Photovoltaic module-integrated stand-alone single-stage switched capacitor inverter with maximum power point tracking," *IEEE Transactions on Power Electronics*, vol. 32, no. 5, pp. 3571–3584, May 2017, doi: 10.1109/TPEL.2016.2587118.

BIOGRAPHIES OF AUTHORS

Jnanaranjan Nayak 🆔 🔗 SC 🔘 received equivalent B.Tech. degree in Electrical Engineering, from The Institutions of Engineers, India, in 2002 and M.Tech. from Berehmpur University, Odisha, India in 2013. Now, he working as a Research Scholar in Electrical Engineering at Kalinga University, Raipur, Chhatisgarha. He can be contacted at email: nayakjnanaranjan@gmail.com.

Sunil Kumar 🆔 🔗 SC 🔘 received his M.Tech. degree from NIT Jamshedpur in 1993 and Ph.D. degree from state government university, in 2002. Now he is working as professor in Kalinga University, Raipur, India. Previously, he has hold key positions in various reputed organization like Birla Engineering College, Dehradun University and Sri Sai University. He can be contacted at email: sunil.Kumar@kalingauniversity.ac.in.

Pradeep Kumar Sahu 🆔 🔗 SC 🔘 is working as an associate professor in the School of Electrical Sciences, KIIT University, Bhubaneswar. He received a Ph.D. degree from the National Institute of Technology, Rourkela in 2015. His research interests are grid-connected PV systems, electric vehicles, power quality, advanced power electronics converters, and soft-computing. He can be contacted at email: pksahu.nitrkl@gmail.com.

Satyaranjan Jena 🆔 🔗 SC 🔘 is currently working as assistant professor in School of Electrical Engineering, KIIT Deemed to be University, Bhubaneswar, Odisha. He has teaching experience of 15 years and research experience of 7 years. His current research interests includes grid integartion of renewables, soft computing, and power electronics. He can be contacted at email: srj.kiit@gmail.com.